JOURNAL OF SOLID STATE CHEMISTRY 57, 135–142 (1985)

# Structures of Niobium and Tantalum Oxide Fluorides Containing Lone-Pair Ions

## I. $Pb_3M_4O_{12}F_2$ ($M$ = Nb or Ta): A Structure with Recognizable Pyrochlore Units

ÖRJAN SÄVBORG AND MONICA LUNDBERG

*Department of Inorganic Chemistry, Arrhenius Laboratory, University of Stockholm, S-106 91 Stockholm, Sweden*

Received December 30, 1983

The tetragonal structure of $Pb_3M_4O_{12}F_2$ ($M$ = Nb or Ta) has been determined and refined from single crystal X-ray diffractometer data to an R value of 0.064. The unit cell parameters are $a_{Nb}$ = 12.6595(3) Å and $c_{Nb}$ = 7.4524(4) Å, and the space group is $P4_2/mnm$. The parameters for the isomorphous tantalum phase are very similar. The structure is built up of corner-sharing $M(O,F)_6$ octahedra in such a way that cavities and tunnels arise, which contain the divalent lead atoms. The coordination numbers at these sites are 5 + 3 and 8, respectively. Bond strength calculations suggest that some of the anion sites are occupied predominantly by fluorine. The relationships with the pyrochlore and fluorite structures are discussed. 

## Introduction

Since the early 1950s several studies of the phase relationships in the system PbO–$Nb_2O_5$ have been performed. A phase with the composition $PbNb_2O_6$ was reported by Goodman (*1*) to have orthorhombic symmetry and ferroelectric properties. Later Francombe (*2*) described a low-temperature rhombohedral modification of $PbNb_2O_6$ and revised the unit cell parameters for the ferroelectric phase which he proposed to be structurally related to the tetragonal tungsten bronze type (*3*). This relation was confirmed by Labbé *et al.* (*4*), who also elucidated the complicated superstructure.

Several phases discovered in the system have structures that are more or less related to pyrochlore. Cook and Jaffe found two phases: the rhombohedral $Pb_2Nb_2O_7$ (*5*) and the cubic $Pb_{1.5}Nb_2O_{6.5}$ (*6*). A number of investigators later indexed $Pb_2Nb_2O_7$ as having an $a$ axis twice as large as the one suggested by Cook and Jaffe. A comprehensive survey of the PbO–$Nb_2O_5$ phase diagram was published by Roth (*7*), although some of his powder patterns were not fully indexed. One of the proposed phases was assigned the formula $Pb_{2.5}Nb_2O_{7.5}$. Kemmler-Sack and Rüdorff (*8*) also suggested the existence of a rhombohedral phase with a composition somewhere between those of $Pb_2Nb_2O_7$ and $Pb_{2.5}Nb_2O_{7.5}$. In this region, Bernotat-Wulf and Hoffmann (*9*) found two phases besides $Pb_2Nb_2O_7$, namely, $Pb_{2.31}Nb_2O_{7.31}$ and $Pb_{2.44}Nb_2O_{7.44}$, and determined the crystal structures. Saine *et al.* (*10, 11*) characterized a number of other compounds belonging to this family of structures. They can be classified as pyrochlore structures containing



0022-4596/85 $3.00

TABLE I

CRYSTALLOGRAPHIC DATA FOR $Pb_3M_4O_{12}F_2$

| | $M$ = Nb | $M$ = Ta |
|---|---|---|
| Unit cell | $a$ = 12.6595(3) Å | $a$ = 12.6639(3) Å |
| | $c$ = 7.4524(4) Å | $c$ = 7.4375(4) Å |
| Space group | $P4_2/mnm$ (No. 136) | |
| Unit cell content | $Z$ = 4 | |
| Density | | |
| calc | 6.80 g cm$^{-3}$ | 8.77 g cm$^{-3}$ |
| obs | 6.78 g cm$^{-3}$ | — |

periodic crystallographic shear planes. The ordering of such planes has been studied using electron diffraction and lattice image techniques (*11*).

As can be seen, a variety of structure types are found in the Pb–Nb–O system. Moreover, phase transitions occur in the compound $PbNb_2O_6$ when the temperature is changed. In order to learn whether fluorine can substitute for oxygen and what effect this exchange may have on structures and properties, we started phase analysis studies on the systems $PbO–PbF_2–M_2O_5–MO_2F$ ($M$ = Nb(12) or Ta(13)). The investigation revealed several phases, including one with the composition $Pb_3M_4O_{12}F_2$. The niobium and tantalum phases proved to be isostructural, but the present work mostly deals with the niobium phase due to difficulties obtaining good single crystals of the Ta phase.

A plausible ordering of oxygen and fluorine on the anion sites is derived. The relation of the structure to the fluorite and pyrochlore types is also discussed.

## Experimental

A sample of the niobium compound was prepared at 1025 K as described in an earlier article (*12*). The unit cell dimensions derived from the powder pattern are given in Table I. A crystal fragment was selected from the sample, and oscillation and Weissenberg photographs indicated that it was a single crystal with Laue symmetry $4/mmm$. The systematic absences $0kl$ for $k + l = 2n + 1$ point to the space groups $P4_2nm$ (No. 102), $P\bar{4}n2$ (No. 118), and $P4_2/mnm$ (No. 136). Intensity data were collected on a PW 1100 automatic four-circle diffractometer. Details of the data collection and the crystal are given in Table II. Corrections for Lorentz, polarization, and absorption effects were applied.

Crystals of the corresponding tantalum compound were prepared in an analogous manner. The powder pattern was very similar to that published in (*12*), and the unit cell parameters are shown in Table I. All examined crystals were twinned, and efforts to obtain a single crystal through cutting produced only a very irregularly shaped fragment from which intensity data were collected in the same way as for the niobium compound. Corrections for Lorentz and polarization effects were applied, but no absorption correction was performed as the very irregular shape and the high value of the linear absorption coefficient (756 cm$^{-1}$) would have yielded an unreliable result.

## Structure Determination

The space group $P4_2/mnm$ was tentatively chosen since the statistical tests indi-

TABLE II

DETAILS OF DATA COLLECTION

| | |
|---|---|
| Crystal size | 0.06 × 0.06 × 0.06 mm$^3$ |
| Radiation | Mo$K\alpha$, $\lambda$ = 0.7101 Å |
| Absorption coefficient | $\mu$ = 364 cm$^{-1}$ |
| Transmission factors | 0.084–0.223 |
| Extinction coefficient | 0.22(4) |
| Scan type | $\theta$–$2\theta$ |
| Scan speed | 0.015° sec$^{-1}$ |
| Scan width | ±0.60° |
| $2\theta$ range | 3°–70° |
| Number of registered reflections | 1194 |
| Number of reflections with $I > 2\sigma(I)$ used in least-squares refinement | 700 |

TABLE III

FINAL POSITIONAL AND THERMAL PARAMETERS FOR $Pb_3Nb_4O_{12}F_2$

| Atom | Position | $x$ | $y$ | $z$ | $U$ or $U_{11}$[a] | $U_{22}$ | $U_{33}$ | $U_{12}$ | $U_{13}$ | $U_{23}$ |
|---|---|---|---|---|---|---|---|---|---|---|
| Pb(1) | 4 *e* | 0 | 0 | 0.2563(3) | 227(6) | 227(6) | 143(9) | −14(9) | 0 | 0 |
| Pb(2) | 8 *i* | 0.2924(1) | 0.0518(1) | 0 | 163(7) | 177(7) | 272(8) | −23(5) | 0 | 0 |
| Nb(1) | 8 *j* | 0.2977(1) | 0.2977(1) | 0.2524(4) | 66(7) | 66(7) | 132(11) | 3(9) | 5(8) | 5(8) |
| Nb(2) | 8 *i* | 0.2412(3) | 0.5456(2) | 0 | 282(16) | 115(14) | 116(13) | 117(12) | 0 | 0 |
| *X*(1) | 4 *g* | 0.390(2) | −0.390(2) | 0 | 157(70) | | | | | |
| *X*(2) | 16 *k* | 0.301(1) | 0.144(1) | 0.308(2) | 121(29) | | | | | |
| *X*(3) | 4 *f* | 0.094(2) | 0.094(2) | 0 | 101(59) | | | | | |
| *X*(4) | 4 *g* | 0.168(2) | −0.168(2) | 0 | 57(52) | | | | | |
| *X*(5) | 4 *f* | 0.258(2) | 0.258(2) | 0 | 102(57) | | | | | |
| *X*(6) | 8 *i* | 0.110(2) | 0.473(2) | 0 | 93(41) | | | | | |
| *X*(7) | 16 *k* | 0.296(1) | 0.448(1) | 0.188(2) | 111(25) | | | | | |

[a] Anisotropic thermal parameters are given in the form $\exp\{-2\pi^2 \cdot 10^{-4}(h^2a^{*2}U_{11} + k^2b^{*2}U_{22} + l^2c^{*2}U_{33} + hka^*b^*U_{12} + hla^*c^*U_{13} + klb^*c^*U_{23})\}$.

cated a centrosymmetric structure. Comparison of Patterson maps from the two data sets revealed positions for the Pb and Nb(Ta) atoms. Positions for the anions were determined from difference Fourier syntheses. The structures were refined by least-squares methods with isotropic temperature factors for all atoms and unit weights for all reflections. The scattering factors and anomalous scattering parameters were taken from (*14*). All anions were treated as oxygens. The final $R$ values from these refinements were 13% for the niobium compound and 15% for the tantalum phase. The atomic positions were at this stage virtually identical for the two compounds. Due to the lack of absorption correction the structure of the Ta compound was not further refined.

Difference maps indicated anisotropic thermal motion for the metal atoms, and inspection of observed and calculated structure factors showed that some reflexions were affected by extinction. The niobium-containing structure was thus refined with anisotropic thermal parameters on all metal atoms and with an isotropic extinction parameter which yielded a final $R = 0.064$. A subsequent difference map showed no peak corresponding to more than 50% of an oxygen atom. No improvement was achieved by lowering the symmetry, and this was taken as a confirmation of the space group $P4_2/mnm$. The final positional and thermal parameters are given in Table III and some relevant interatomic distances are summarized in Table IV.

TABLE IV

SELECTED INTERATOMIC DISTANCES IN Å FOR $Pb_3Nb_4O_{12}F_2$

| | | | Mean value |
|---|---|---|---|
| Nb(1)–O(4) | | 1.95(1) | |
| –O(7) | 2× | 1.96(1) | |
| –O(2) | 2× | 1.99(1) | |
| –O(5) | | 2.01(1) | 1.98 |
| Nb(2)–O,F(6) | | 1.90(2) | |
| –O(2) | 2× | 1.97(1) | |
| –O(7) | 2× | 1.99(1) | |
| –O(1) | | 2.05(2) | 1.98 |
| Pb(1)–O,F(3) | 2× | 2.55(2) | |
| –O(1) | 2× | 2.68(2) | |
| –O(7) | 4× | 2.70(1) | 2.66 |
| Pb(2)–O,F(6) | | 2.40(2) | |
| –O,F(3) | | 2.57(2) | |
| –O(2) | 2× | 2.58(1) | |
| –O(5) | | 2.65(2) | 2.55 |
| –O(7) | 2× | 2.90(1) | |
| –O(4) | | 3.20(2) | 2.72 |
| $X$–$X_{min}$ | | 2.72(2) | |
| $X$–$X_{max}$ | | 2.87(2) | |

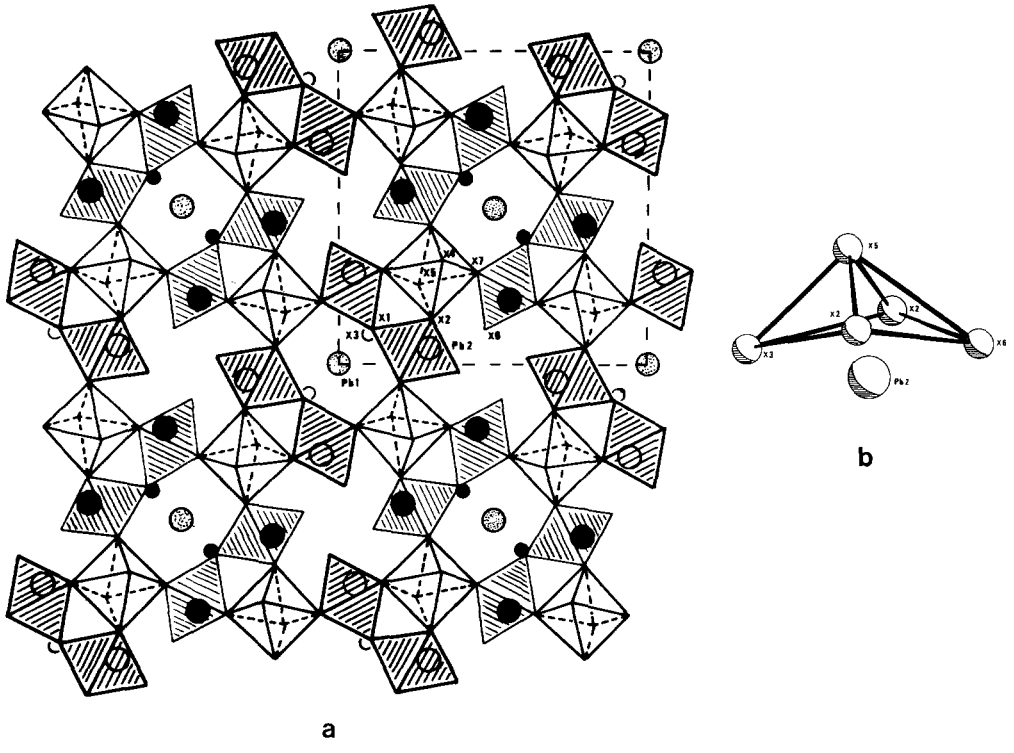


FIG. 1. (a) The structure of $Pb_3Nb_4O_{12}F_2$ projected along the $c$ axis. The octahedra, shaded in fine and bold lines, contain Nb atoms situated at $z = 0$ and $z = \frac{1}{2}$, respectively. The nonshaded octahedra correspond to Nb atoms at $z \sim \pm 0.25$. The large circles, empty, shaded, and filled, represent Pb atoms at $z = 0$, $z \sim \pm 0.25$ and $z = \frac{1}{2}$. The small, empty and filled circles correspond to $X$ atoms at $z = 0$ and $z = \frac{1}{2}$, respectively. (b) A detailed drawing of the coordination polyhedron of Pb(2).

## Description

The structure of $Pb_3Nb_4O_{12}F_2$, projected along [001] in Fig. 1, may be described as a framework of $NbX_6$ octahedra with the net composition $Nb_4X_{13}$, into which three Pb atoms and one extra $X$ atom are inserted ($X$ = O,F).

The framework can be regarded as based on identical groups of four mutually corner-sharing octahedra (cf. Fig. 2a). These groups are composed of two non-equivalent pairs of octahedra (marked I and II in Fig. 2a). The groups are connected to each other by common $X$ vertices to form infinite staggered strings of type I octahedra, running parallel to the $c$ axis. As a consequence of this linking, cavities arise between the pairs of type II octahedra. Such cavities are filled with two-thirds of the Pb atoms (cf. Fig. 2a). The columns thus formed are connected by corner sharing to create infinite tunnels which accommodate the remaining one-third of the Pb atoms. Furthermore, the extra $X$ atoms are inserted two by two at the same height and located at opposite sides of the tunnels (displayed as small, empty, and filled circles in Fig. 1a). However, due to the way the columns are arranged, one outward $X$ atom in each octahedron of type II is not engaged in corner sharing. Four rows of such $X$ atoms form tunnels comprising vacant, tetrahedral cavities centered at the midpoints of the $a$ axes.

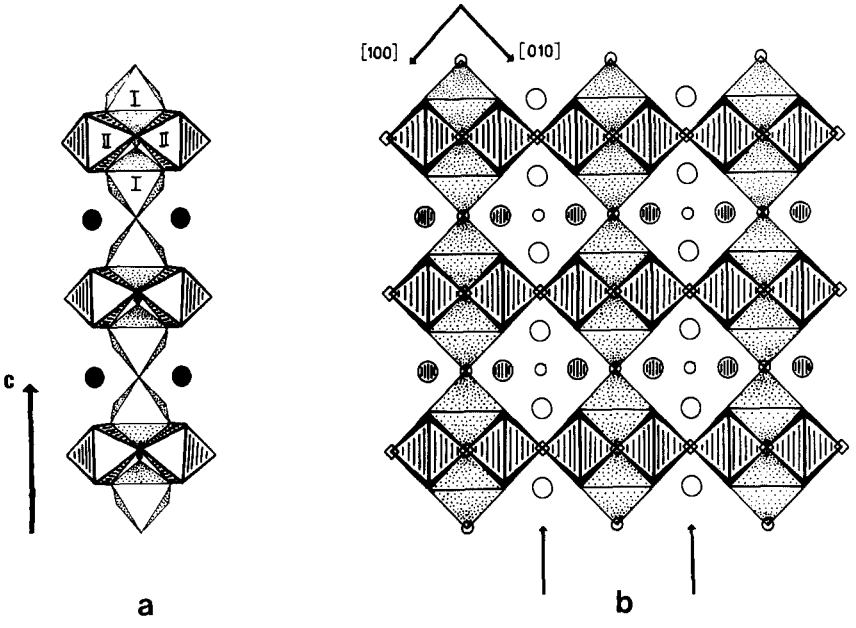


FIG. 2. (a) The pyrochlore column (*PyC*) in the compound $Pb_3Nb_4O_{12}F_2$ projected along [110]. Filled circles represent Pb atoms at the same height as the Nb atoms in the heavily shaded octahedra. I and II identify the two nonequivalent pairs of octahedra. (b) A $\frac{1}{2}$ [001] projection of the ideal pyrochlore structure. $NbX_6$ octahedra drawn in fine and bold lines represent Nb atoms at $z = 0$ and $\frac{1}{4}$. Large, empty and shaded circles correspond to Pb atoms at $z = 0$ and $\frac{1}{4}$. Squares indicate anions removed from the fluorite structure in order to transform it to pyrochlore. Small circles denote the half-occupied anion site in $Pb_{1.5}Nb_2O_{6.5}$ (*9*).

The Nb atoms are all octahedrally coordinated, with bond distances ranging from 1.898 to 2.053 Å. The average is 1.979 Å, in very good agreement with 1.982 Å found in $Pb_{1.5}Nb_2O_{6.5}$ (*9*). The coordination polyhedra of eight $X$ atoms around Pb(1) form somewhat distorted cubes sharing opposite edges in such a way that the face diagonals of the cubes are parallel to the $c$ axis. The Pb(1)–$X$ distances vary between 2.55 and 2.70 Å, resulting in two alternating Pb(1)–Pb(1) distances (3.820 and 3.632 Å).

The Pb(2) atom has eight neighboring $X$ atoms at distances within the interval 2.40 to 3.20 Å. The five nearest of these within 2.65 Å are arranged as a distorted square pyramid with the Pb atom slightly below the base (cf. Fig. 1b). The remaining $X$ atoms are situated on the other side of Pb(2) at distances varying from 2.90 to 3.20 Å. Such one-sided coordination around lead is quite common due to the electrostatic repulsion from the lone pair (*15*).

No indication of ordering of the O and F atoms was observed during the refinement. The calculation of bond strength sums, however, offers an opportunity to analyze the distribution of oxygen and fluorine over the anion sites. Pauling (*16*) originally defined the strength of a bond as the valency of the central atom divided by its coordination number. This concept requires that the bonds surrounding an atom are of equal length and also that the coordination number can be accurately established. In the present structure the coordinations around Nb(1), Nb(2), and Pb(1) fulfill both requirements reasonably well, but this is unfortunately not the case for Pb(2). Here the scatter in bond distances is considerable, and

there is no sharp limit to the coordination number. If, however, empirical bond length–bond strength curves of the type published by Brown and Shannon (*17*) are used, the absence of a well-defined coordination number causes no problem. Parameters for such curves for Nb–O and Pb–O bonds have been published by Brown and Kang Kun Wu (*18*), and these were used to calculate bond strength sums around all atoms in the structure. The result of these calculations, summarized in Table V, indicates that the positions *X*(1), *X*(2), *X*(4), *X*(5), and *X*(7) are occupied by oxygen. The eight fluorine atoms in the unit cell are thus probably distributed over the fourfold position *X*(3) and the eightfold position *X*(6). If *X*(3) is fully occupied by fluorine and if *X*(6) has one-half O and one-half F character, the resulting bond strength sums should ideally be 1.0 and 1.5, respectively. This model compares favorably with the values in Table V, but as it is not obvious that parameters for bonds to oxygen can also be used for bonds to fluorine, such a conclusion may be unwarranted.

TABLE V

BOND STRENGTH SUMS FOR $Pb_3Nb_4O_{12}F_2$ CALCULATED WITH PARAMETERS FROM REF. (*18*)

| Atom | $\Sigma s_{calc}$ |
|---|---|
| Pb(1) | 1.9 |
| Pb(2) | 1.9 |
| Nb(1) | 5.0 |
| Nb(2) | 5.0 |
| *X*(1) | 1.8 |
| *X*(2) | 1.9 |
| *X*(3) | 1.2 |
| *X*(4) | 2.0 |
| *X*(5) | 2.0 |
| *X*(6) | 1.4 |
| *X*(7) | 2.0 |

## Structural Relationships

The columns used to describe the structure of $Pb_3Nb_4O_{12}F_2$ bear interesting relationships to structural elements in pyrochlore as well as in fluorite. Among lead compounds, the structure of the high-temperature form of $PbF_2$ is of the fluorite type (*22*), while a number of lead niobates possess structures closely related to pyrochlore.

It was pointed out by Aleshin and Roy (*19*) that the pyrochlore structure may be derived from the fluorite structure by removing one-eighth of the anions as shown in Fig. 2b. The vacant anion sites are indicated by squares. The compound $Pb_{1.5}Nb_2O_{6.5}$ (*9*) has the undistorted cubic unit cell with $\frac{3}{4}$ occupancy of the lead position and $\frac{1}{2}$ occupancy of the oxygen site, encircled in Fig. 2b. Unidimensionally infinite columns can be distinguished, as shown schematically in Fig. 2a. The columns are constructed from the pyrochlore building unit of four corner-sharing octahedra (*20*) interleaved by Pb atoms, and will be referred to here as "the pyrochlore column" (*PyC*). A *PyC* projected along the infinite direction is shown in Fig. 3a. The relation between the structure of the present compound and the pyrochlore type can easily be demonstrated by using these *PyC* units as is shown in Figs. 3b and c.

The unit cell of $Pb_3Nb_4O_{12}F_2$ contains four *PyC* related by $\pi/2$ rotation and $\frac{1}{2}\,\vec{c}$ translation, as is obvious from Fig. 3b.

The pyrochlore structure viewed along $[110]_P$ shows linking of *PyC*. In this case, however, translations are required only to generate the structure. The six-sided tunnels in both structures are filled with the Pb and *X* atoms corresponding to the rows, marked with arrows in Fig. 2b, which separate the columns.

As previously mentioned, the compound $Pb_{1.5}Nb_2O_{6.5}$ has the pyrochlore structure (space group $Fd\bar{3}m$, origin at the center of $\bar{3}m$) with 50% occupancy of the oxygen site

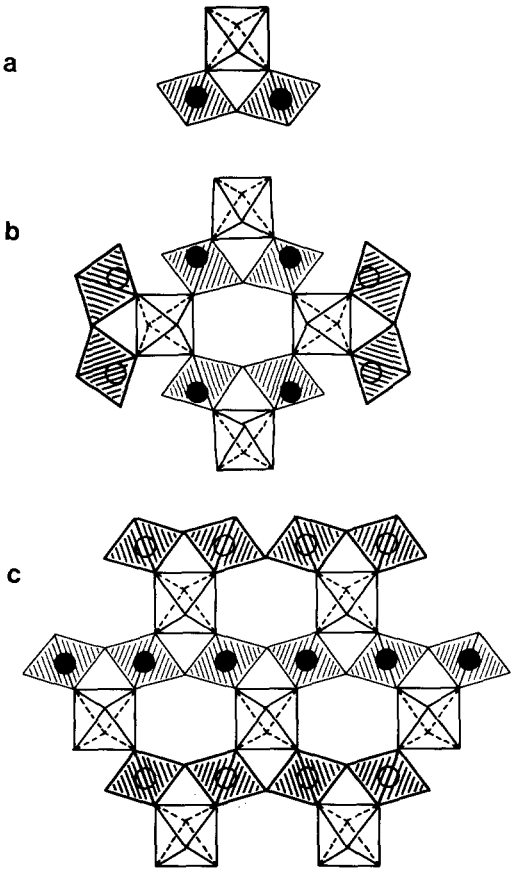


FIG. 3. (a) Pyrochlore column (*PyC*) projected along the infinite direction. (b) Framework of the $Pb_3Nb_4O_{12}F_2$ structure projected along [001]. The *PyC*'s are rotated through $\pi/2$ radians and translated $\frac{1}{2}\vec{c}$ relative to each other. (c) Framework of the pyrochlore structure viewed along [110] emphasize the *PyC* arrangement.

(8a) in the tunnel. A composition with this position fully occupied could be achieved by substitution of fluorine for oxygen. The result would be the composition $Pb_{1.5}Nb_2O_6F$, which is actually the composition of the present phase. The reason for this compound not having the pyrochlore structure can be understood from calculations of the bond strength sums around the Pb atom. If the anion site is fully occupied the coordination number of Pb is 8. The valence of the Pb atom would then become 2.3, and it would thus be quite overbonded. In $Pb_{1.5}Nb_2O_{6.5}$ the half occupancy of the anion tunnel site results in an average coordination number of $7\frac{1}{3}$, and the calculated valence would be 2.0 in good agreement with the expected value.

The *PyC* concept can be extended to the structure of $\beta$-$Na_2Ta_2O_5F_2$ (*21*) (cf. Fig. 4). The compound contains more fluorine per transition metal than $Pb_{1.5}Nb_2O_6F$, but the ratio of anion to transition metal remains the same. $\beta$-$Na_2Ta_2O_5F_2$ has a structure similar to that of pyrochlore, with the difference that the metal atom positions are shifted by $\frac{1}{2}\vec{b}$ in one of the Na–Ta sequences in every second *PyC* unit. This arrangement contains $TaX_6$ octahedra having one or two unshared corners.

Bond strength sums were calculated for all atoms in order to investigate the possibility of specific anion sites where fluorine could be located. The result is shown in Table VI. The anion sites 1, 3, and 9 have significantly lower bond sum values than the rest of the sites and can be assumed to be mainly occupied by fluorine. These sites can, at most, contain 12 out of the 16 fluorine atoms in the unit cell, and the rest of

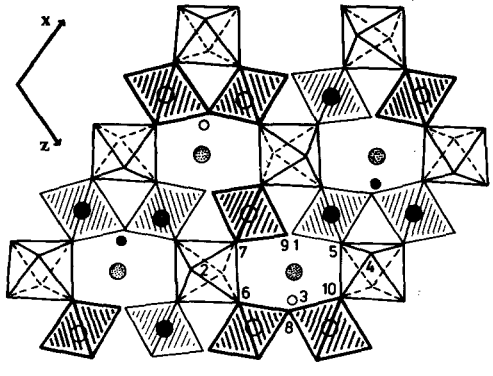


FIG. 4. The structure of $\beta$-$Na_2Ta_2O_5F_2$ projected along the $b$ axis. The octahedra shaded in fine and bold lines contain Ta atoms located at $y = 0$ and $\frac{1}{2}$, respectively. The nonshaded octahedra correspond to Ta atoms at $y = \pm\frac{1}{4}$. The large circles, empty, shaded, and filled, represent Na atoms at $y = 0$, $\pm\frac{1}{4}$, and $\frac{1}{2}$. The small, empty and filled circles correspond to $X$ atoms at $y = 0$ and $\frac{1}{2}$, respectively.

TABLE VI

BOND STRENGTH SUMS FOR $\beta$-$Na_2Ta_2O_5F_2$ BASED ON PARAMETERS FROM REFS. (*18, 21*)

| Atom | $\Sigma s_{calc}$ |
|---|---|
| Ta(1) | 5.3 |
| Ta(2) | 4.9 |
| Ta(3) | 5.1 |
| Ta(4) | 5.0 |
| Ta(5) | 5.3 |
| Na(1) | 1.2 |
| Na(2) | 1.2 |
| Na(3) | 1.2 |
| Na(4) | 1.2 |
| *X*(1) | 1.3 |
| *X*(2) | 1.9 |
| *X*(3) | 1.2 |
| *X*(4) | 1.9 |
| *X*(5) | 2.0 |
| *X*(6) | 1.9 |
| *X*(7) | 2.0 |
| *X*(8) | 2.1 |
| *X*(9) | 1.2 |
| *X*(10) | 1.9 |

the fluorines are probably distributed in a disordered manner.

Interesting features can be observed by comparing the structures and bond strength calculations of the compounds $Pb_{1.5}Nb_2O_6F$ and $\beta$-$Na_2Ta_2O_5F_2$. Those anion sites that are favorable for fluorine atoms are not involved in corner sharing between $NbX_6$ or $TaX_6$ octahedra. In both structures *X*(3) is an anion tetrahedrally coordinated by Pb or Na, while *X*(1) and *X*(9) in the Na compound have features similar to those of *X*(6) in the Pb compound.

## Acknowledgments

We thank Professor Arne Magnéli for his encouraging interest and for stimulating discussions. We are also indebted to Professor Lars Kihlborg for his continuous support and for valuable comments on the manuscript. This study has been carried out within a research program supported by the Swedish Natural Research Council.

## References

1. G. GOODMAN, *J. Amer. Ceram. Soc.* **36,** 368 (1953).
2. M. H. FRANCOMBE, *Acta Crystallogr.* **9,** 683 (1956).
3. A. MAGNÉLI, *Ark. Kemi* **1,** 213 (1949).
4. PH. LABBÉ, M. FREY, B. RAVEAU, AND J. C. MONIER, *Acta Crystallogr. B* **33,** 2201 (1977).
5. W. R. COOK, JR., AND H. JAFFE, *Phys. Rev.* **88,** 1426 (1952).
6. W. R. COOK, JR., AND H. JAFFE, *Phys. Rev.* **89,** 1297 (1953).
7. R. S. ROTH, *J. Res. Natl. Bur. Stand.* **62,** 27 (1959).
8. S. KEMMLER-SACK AND W. RÜDORFF, *Z. Anorg. Allg. Chem.* **344,** 23 (1966).
9. H. BERNOTAT-WULF AND W. HOFFMANN, *Z. Kristallogr.* **158,** 101 (1982).
10. M. C. SAINE, R. CHEVALIER, AND H. BRUSSET, *C. R. Acad. Sci. Paris* **284,** 331 (1977).
11. M. C. SAINE, G. SCHIFFMACHER, M. GASPERIN, AND H. BRUSSET, *Rev. Chim. Mineral.* **16,** 597 (1979).
12. Ö. SÄVBORG AND M. LUNDBERG, *Mater. Res. Bull.* **15,** 1433 (1980).
13. Ö. SÄVBORG, I. ELGENMARK, AND M. LUNDBERG, to be published.
14. *International Tables for X-Ray Crystallography,* Vol. IV, Kynoch Press, Birmingham (1974).
15. K. KATO, I. KAWADA, AND K. MURAMATSU, *Acta Crystallogr. B* **30,** 1634 (1974).
16. L. PAULING, *J. Amer. Chem. Soc.* **51,** 1010 (1929).
17. I. D. BROWN AND R. D. SHANNON, *Acta Crystallogr. A* **29,** 226 (1973).
18. I. D. BROWN AND KANG KUN WU, *Acta Crystallogr. B* **32,** 1957 (1976).
19. E. ALESHIN AND R. ROY, *J. Amer. Ceram. Soc.* **45,** 18 (1962).
20. H. NYMAN, S. ANDERSSON, B. G. HYDE, AND M. O'KEEFFE, *J. Solid State Chem.* **26,** 123 (1978).
21. M. VLASSE, J.-P. CHAMINADE, J.-C. MASSIER, AND M. POUCHARD, *J. Solid State Chem.* **12,** 102 (1975).
22. A. BYSTRÖM, *Ark. Kemi Mineral. Geol.* **24A,** No. 33 (1947).